Supplemental Information

The Gene-Silencing Protein MORC-1 Topologically

Entraps DNA and Forms Multimeric Assemblies

to Cause DNA Compaction

HyeongJun Kim, Linda Yen, Somsakul P. Wongpalee, Jessica A. Kirshner, Nicita Mehta, Yan Xue, Jonathan B. Johnston, Alma L. Burlingame, John K. Kim, Joseph J. Loparo, and Steve E. Jacobsen
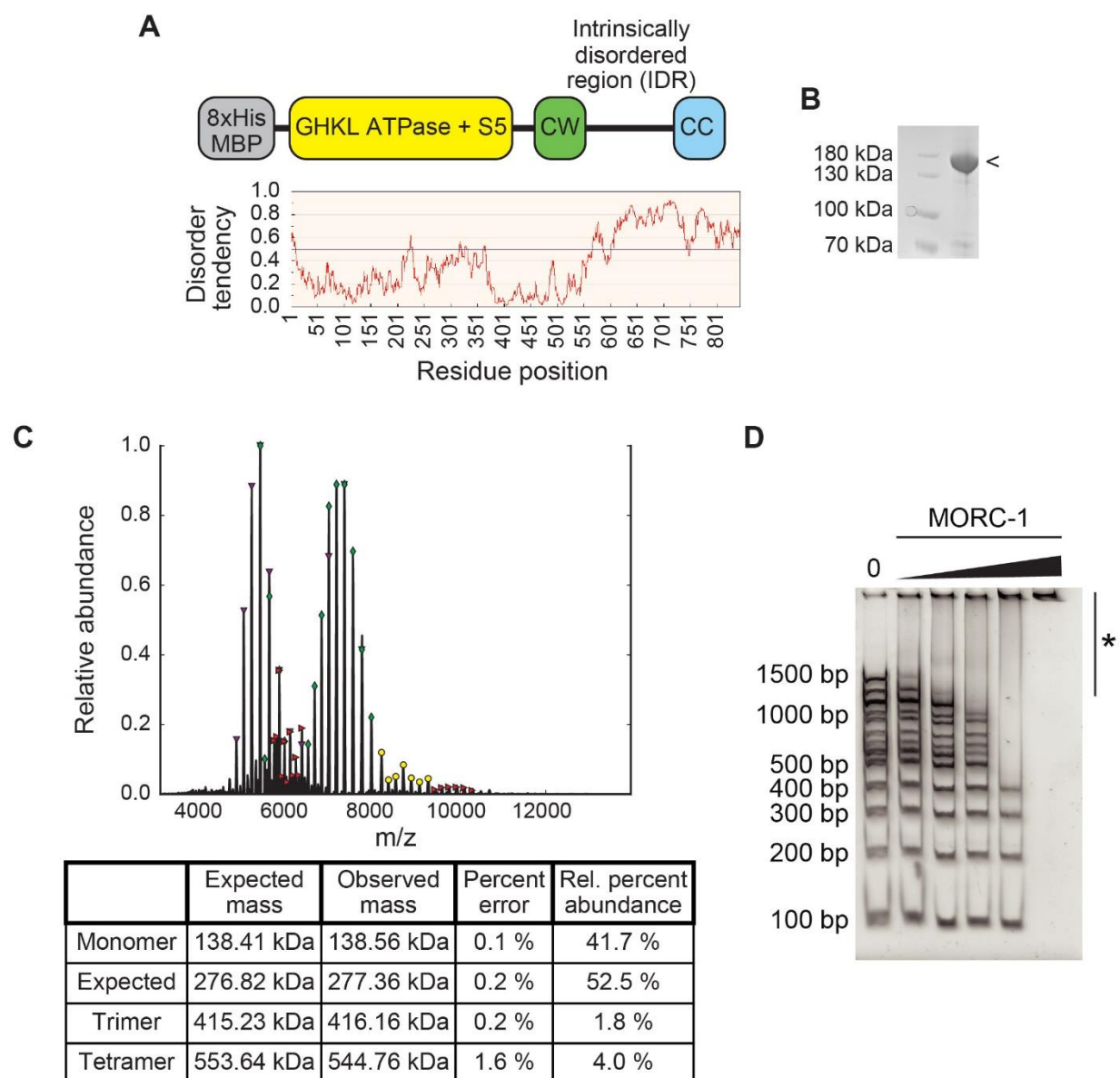
A

8xHis MBP | GHKL ATPase + S5 | CW | Intrinsically disordered region (IDR) | CC

Disorder tendency vs Residue position

B

180 kDa
130 kDa
100 kDa
70 kDa

C

Relative abundance vs m/z

	Expected mass	Observed mass	Percent error	Rel. percent abundance
Monomer	138.41 kDa	138.56 kDa	0.1 %	41.7 %
Expected	276.82 kDa	277.36 kDa	0.2 %	52.5 %
Trimer	415.23 kDa	416.16 kDa	0.2 %	1.8 %
Tetramer	553.64 kDa	544.76 kDa	1.6 %	4.0 %

D

MORC-1

0

1500 bp
1000 bp
500 bp
400 bp
300 bp
200 bp
100 bp

*

Figure S1. MORC-1 Native Mass Spectrometry. (Related to Figure 1).

(A) Cartoon schematic of the MORC-1 construct. Protein fusion contains an N terminal 8x Histidine tag and a maltose binding protein (MBP) solubility tag. The catalytic ATPase module is comprised of the GHKL ATPase domain and the S5 fold (S5). MORC-1 also contains a CW domain (CW) in addition to a C terminal coiled coil (CC) domain. IUPRED2A analysis indicates that MORC-1 possesses a disordered region.

(B) Coomassie gel of purified 8xHis-MBP-MORC-1 protein. "<" denotes protein.

(C) MORC-1 can form multimers. Native mass spectrum of overlapping charge states that correspond to MORC-1 monomer, dimer, trimer, and tetramer. The charge envelope for the monomer is represented by purple triangles, dimer by green diamonds, trimer by yellow circles, and tetramer by red triangles. Accompanying table reports the measured and expected masses in kilodaltons (kDa), and relative abundance in the sample.

(D) Protein ([MORC-1] = 200 nM, 400 nM, 800 nM, 1.6 μM, 3.2 μM) was incubated with a double stranded DNA ladder. Complexes were resolved on a 5% native acrylamide gel and visualized using SyBr Gold staining. Asterisk (*) denotes MORC-1 DNA complexes
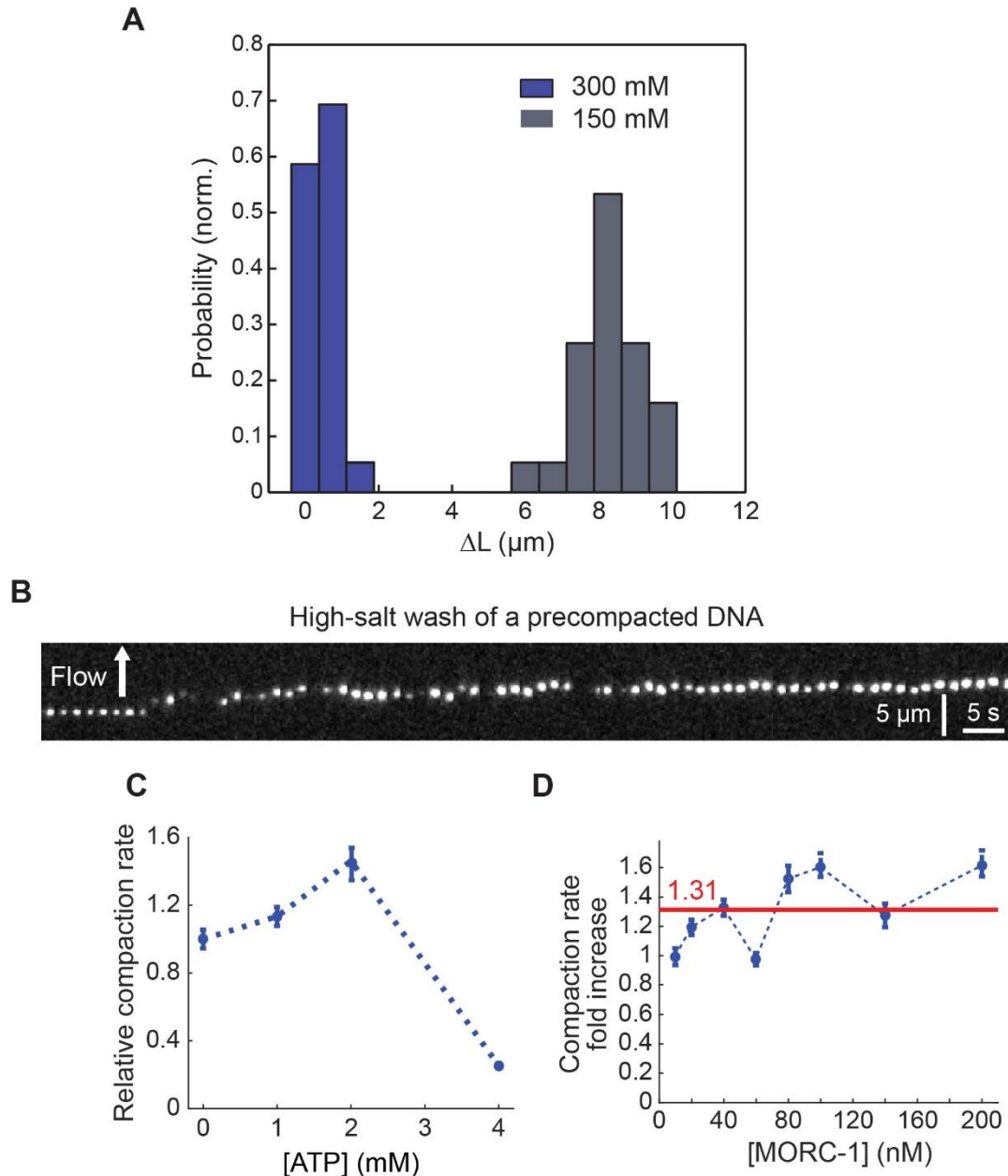
Figure S2. MORC-1 compaction is nucleotide responsive. (Related to Figure 2).

(A) MORC-1 compaction does not robustly occur in 300 mM NaCl or above. Histogram analyzing n=25 compaction events in 150 mM and 300 mM NaCl.

(B) Kymograph showing that compaction is partially reversible. [MORC-1]= 60 nM, [ATP] = 2 mM. Pre-compacted DNA was subjected to a high salt wash (containing 500 mM NaCl, 2 mM $MgCl_2$, 2 mM ATP). Scale bar represents 5 seconds and 5 μm.

(C) MORC-1 compaction rate is responsive to ATP concentration. Relative compaction rates were measured using 100 nM of MORC-1. n=86, 93, 55, 51 for [ATP] = 0, 1, 2, 4 mM, respectively. The error bars (SE) were calculated using the error propagation formula. The observed drop in compaction rate is likely due to substrate inhibition.

(D) ATP stimulates DNA compaction. The ratios of compaction rates in the presence of ATP to those in the absence of ATP were calculated. The error bars (SE) were calculated using the error propagation formula.
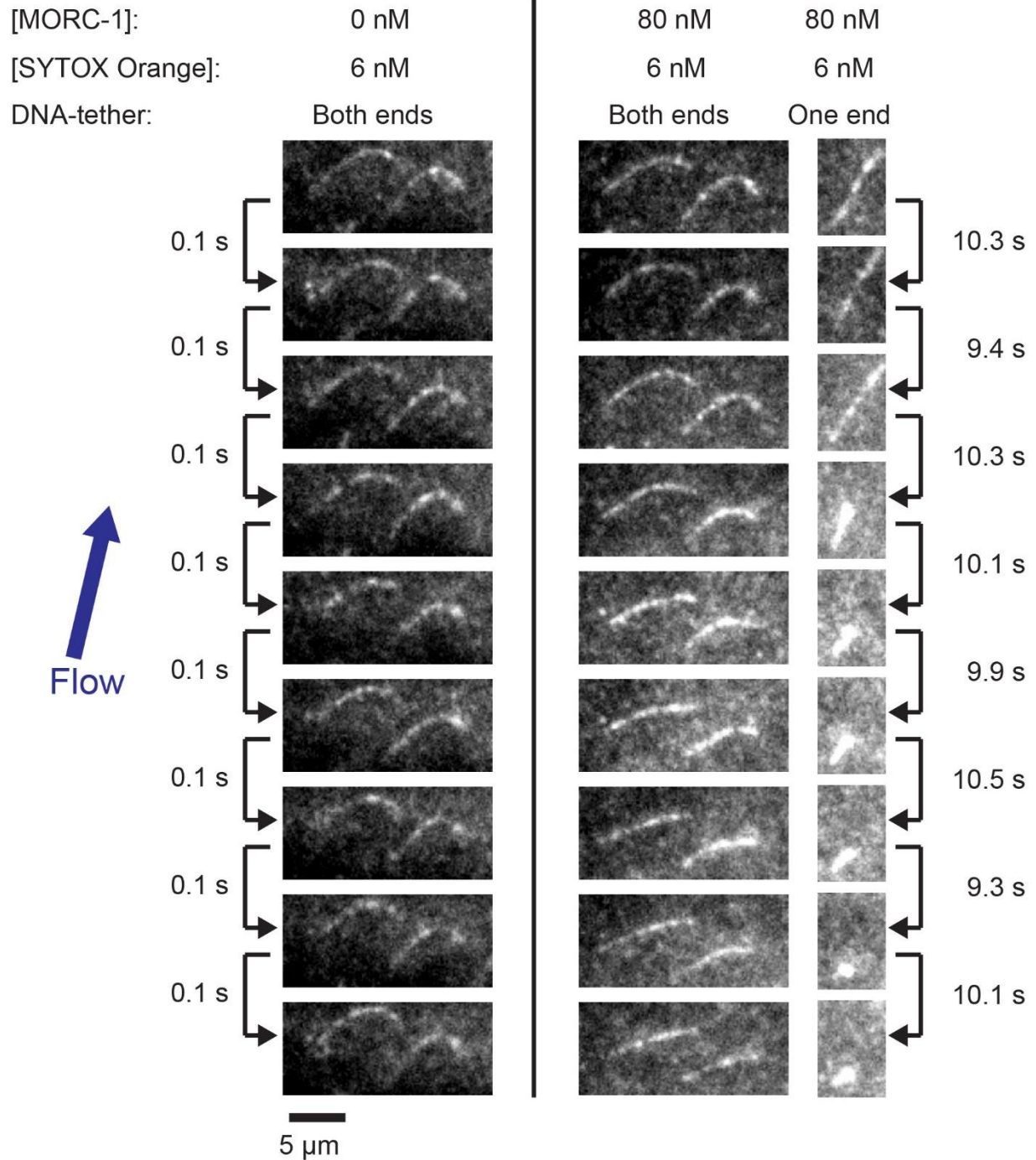
Figure S3. MORC-1 compacts doubly-tethered DNA without actively extruding a loop. (Related to Figure 2 and Video S1).

Slack, doubly tethered DNA was subjected to orthogonal flow and stained with SYTOX Orange. Upon adding MORC-1, double tethered DNA became taut, indicating the presence of DNA compaction without large looping events. Single tethered DNA in the same field of view compacted down to the tether point. Experiment was conducted in the presence of 2 mM ATP.
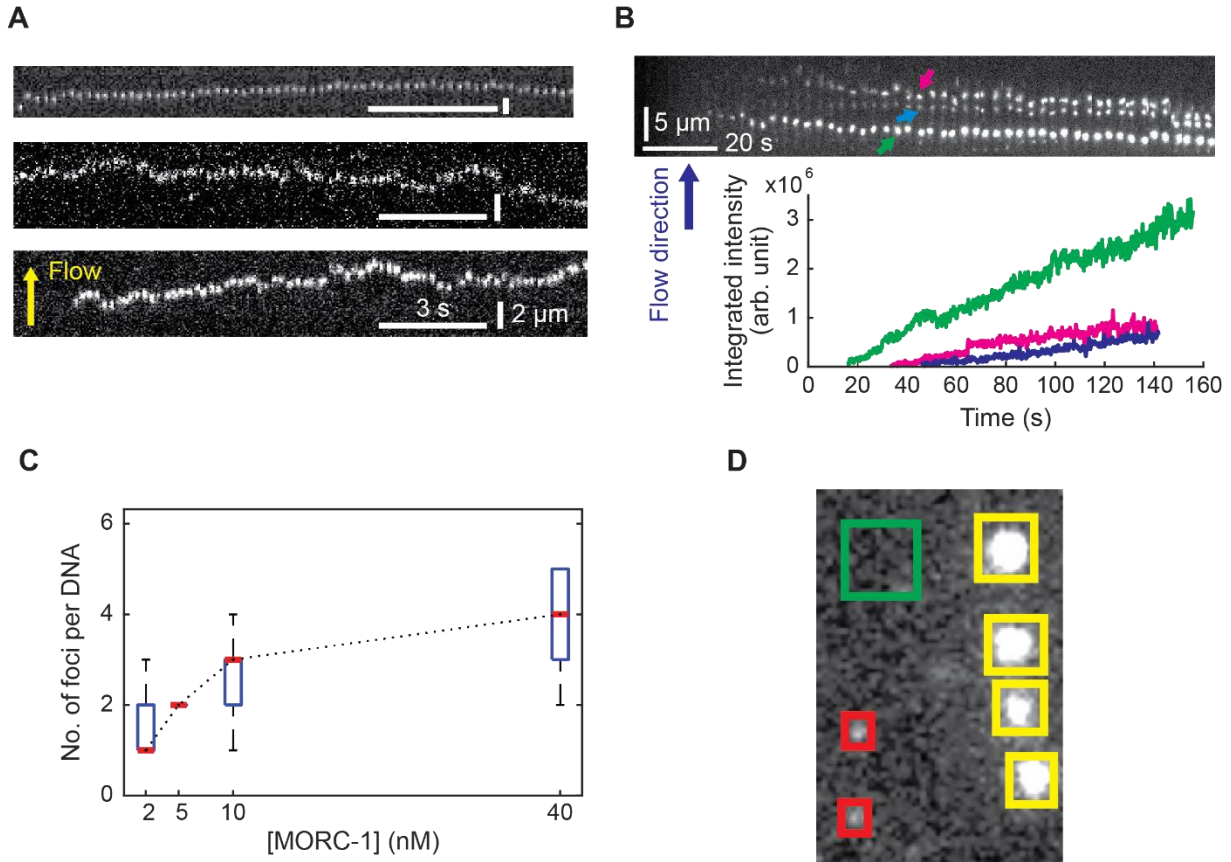
**Figure S4. MORC-1 can diffuse along DNA and form foci.
(Related to Figure 3 and Videos S2 and S3).**

(A) Three examples showing MORC-1 diffusion along flow-stretched DNA at low MORC-1 concentration. The MORC-1 concentration for the top panel is 1 nM, and 2 nM for the middle and the bottom panels. All experiments were performed in the presence of 2 mM ATP. Scale bars correspond to 3 seconds and 2 μm.

(B) MORC-1 forms foci on DNA and focus size increases over time. A representative kymograph and accompanying graph illustrating increases in fluorescent intensity of foci marked by magenta, blue, and green arrows over time. [Cy3-MORC-1] = 40 nM, [ATP] = 2 mM. There is no quantum dot on the DNA.

(C) Box plots showing the number of foci per DNA. Foci were counted 140 seconds after MORC-1 addition. Red line inside each box: Median value. The bottom and top edges of each box: 25th and 75th percentiles. Black dotted lines connecting nearby median values were added for visual guidance.

(D) Method of counting the number of MORC-1 molecules in foci. The net integrated signal intensities for foci (yellow box) were calculated by subtracting integrated background (green box). Likewise, the net integrated signal intensities of single Cy3 (red box) were calculated. The ratio of the net integrated focus signal intensity to that of the single Cy3 is an estimated number of MORC-1 dimers in each focus.
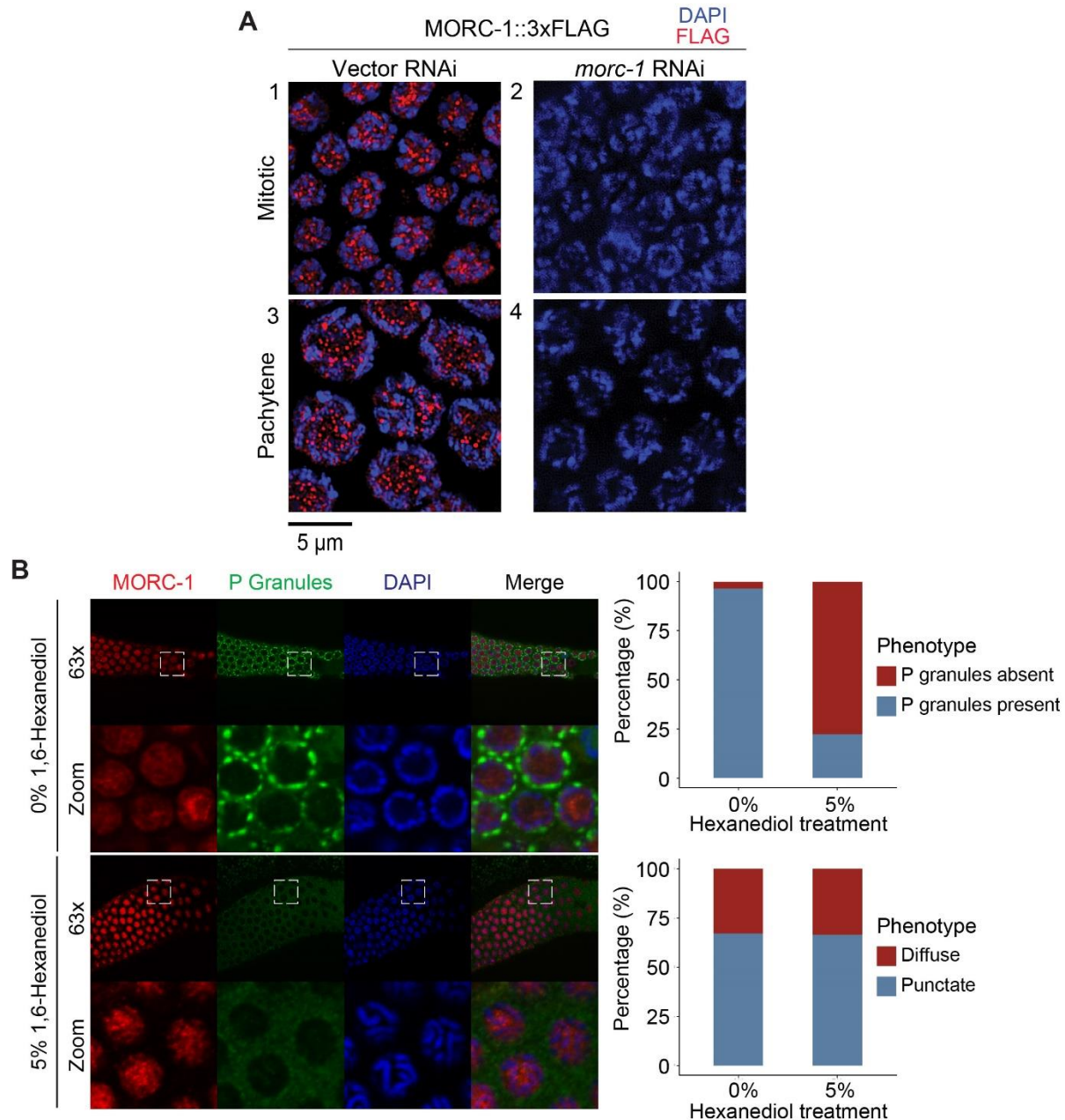
Figure S5. MORC-1 puncta are resistant to dissolution by 1,6 hexanediol. (Related to Figure 4).

(A) Images (single slices) of immunostaining are shown for *C. elegans* mitotic germ cells (1) and pachytene cells (3) expressing MORC-1::3xFLAG. RNAi against *morc-1* abrogates anti-FLAG signal in mitotic cells (2) and pachytene cells (4).

(B) MORC-1 puncta are resistant to dissolution by 1,6-hexanediol. (Left) Single slice images of extruded gonads from *C. elegans* expressing MORC-1::3xFLAG worms are stained with anti-FLAG (red), anti-CSR-1 (green), a P granule marker, and DAPI after incubation in buffer or 5% 1,6-hexanediol. (Upper right) Quantification of the percentage of nuclei with P granules either present or absent in the indicated concentrations of 1,6-hexanediol. n=144 cells for 0% 1,6-hexanediol and n=72 cells for 5% 1,6-hexanediol. p=2.2e-16 (two sample t test). (Lower right) Quantification of the percentage of cells having MORC-1 in a diffuse or punctate state. n=144 cells for 0% 1,6-hexanediol and n=72 cells for 5% 1,6-hexanediol. p=0.9192 (two sample t test). Though the P granules dissolve in 1,6-hexanediol, MORC-1::3xFLAG puncta do not.
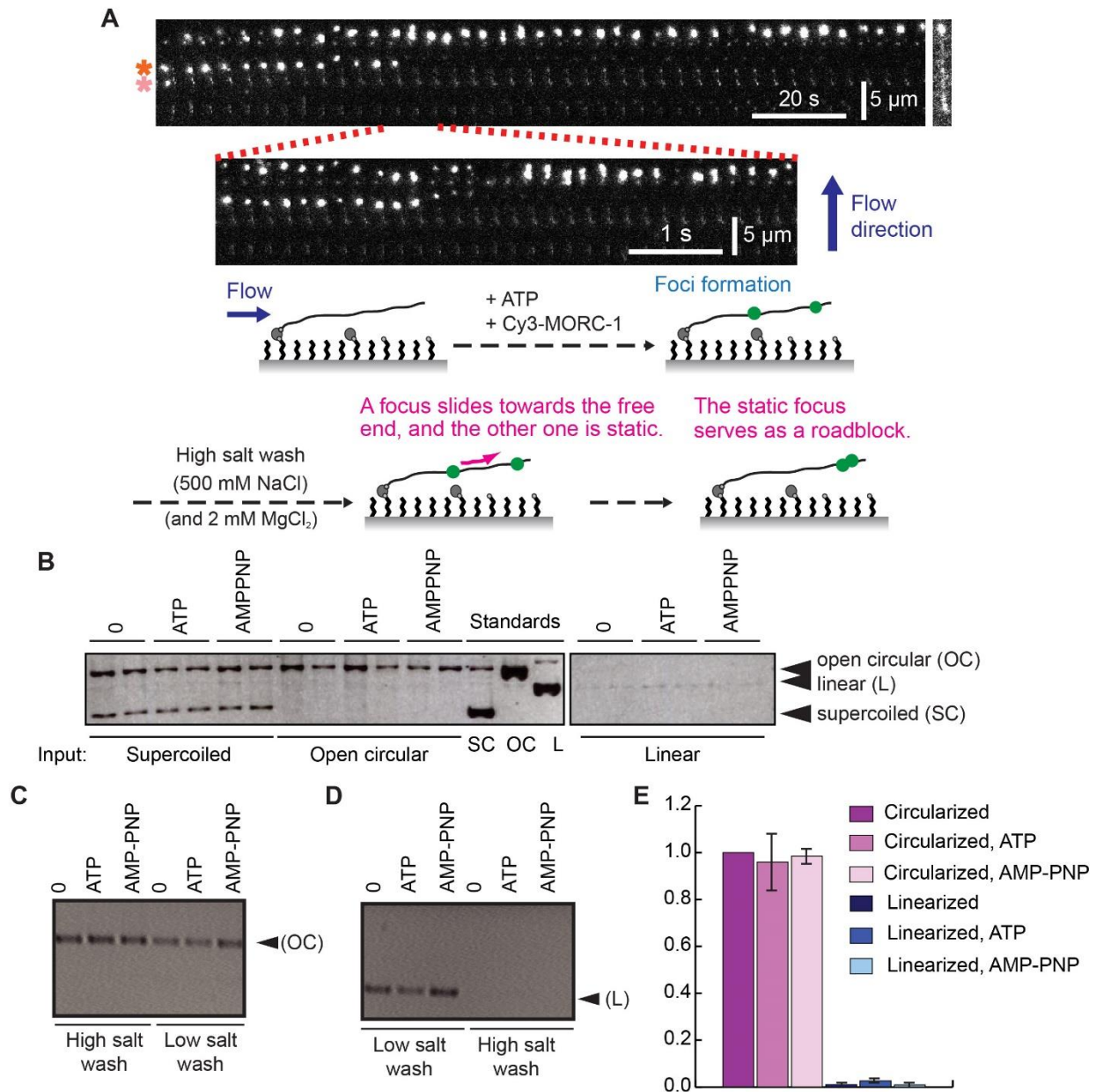
Figure S6. Static MORC-1 foci can block other MORC-1 foci from leaving DNA; entrapment is not nucleotide dependent. (Related to Figures 5 and 6, and Video S7).

(A) Static foci can serve as roadblocks for mobile MORC-1 foci. Representative kymograph demonstrating that MORC-1 focus movement is blocked by a static MORC-1 focus. Foci were pre-formed on DNA by flowing in 10 nM MORC-1 in the presence of 2 mM ATP, then washed with a high salt buffer (500 mM NaCl, 2 mM MgCl$_2$, 2 mM ATP). The top focus (orange asterisk) contains 10 MORC-1 molecules while the bottom focus (peach asterisk) contains 7. Scale bars are 20 seconds and 10 μm (top), and 1 second and 5 μm (bottom).

(B) MORC-1 topological preferences are not nucleotide dependent. 6.4 μM MORC-1 was incubated with 200 ng of various forms of DNA in the presence of 2 mM nucleotide and 4 mM MgCl$_2$, then subjected to a high salt wash (500 mM NaCl). MORC-1 enrichment of open circular or supercoiled forms was similar despite additional nucleotide. Loss of the linear form also occurred regardless of additional nucleotide. Note: the supercoiled stock contained presence of some open circular plasmid.

(C and D) For **(C)** circular DNA and **(D)** linear DNA, addition of nucleotide does not significantly influence MORC-1 binding preferences under low or high salt washes. [MORC-1] = 400 nM.

(E) Quantitation of retention preferences after high salt washes from panel b, c, and d; densitometry was performed using Fiji, then normalized to circular DNA retention without any additional nucleotide. All circular (supercoiled and open circular) samples were considered together. Error bars represent standard error of the mean. Circular n=3; linear n=2.